High Accuracy Wireless Time-Frequency Transfer For Distributed Phased Array Beamforming

Jason M. Merlo[1], Anton Schlegel[2], and Jeffrey A. Nanzer[3]
Electrical and Computer Engineering, Michigan State University, USA
[1]merlojas@msu.edu, [2]schleg19@msu.edu, [3]nanzer@msu.edu

***Abstract*— Wirelessly coordinated distributed arrays will have a significant impact in next generation communications and sensing systems in coming years. However, to achieve high modulation bandwidths and carrier frequencies, timing and frequency transfer must be synchronized to small fractions of the modulation and carrier periods respectively. In this work, we demonstrate coordination and beamforming of a wireless distributed antenna array at $1\,\mathrm{GHz}$ in a cluttered outdoor environment achieving a coherent gain of 95.4% and beamforming accuracy of $27.6\,\mathrm{ps}$ over a $41\,\mathrm{m}$ channel.**

***Keywords*— Clock synchronization, distributed arrays, distributed beamforming, two-way time transfer, radar, remote sensing, wireless sensor networks, wireless synchronization.**

I. Introduction

In recent years, distributed wirelessly coordinated antenna arrays have been gaining interest and have been identified as an enabling technology for next generation systems, ranging from interplanetary communication relays and on-orbit observatories [1, TX08.2.3, TX05.2.6], to planetary remote sensing and imaging [2, TA 5.6.7]. The benefits of distributing the array across multiple nodes are numerous. First, the nodes may be added or removed at any time making it inherently robust to failure—if any one node fails, the rest of the array remains operational. Second, because nodes are no longer fixed, the array can adapt its aperture to meet realtime requirements for a given operation such as operating frequency or sidelobe levels. Third, costs for some applications may be substantially lowered compared to traditional fixed arrays by enabling gain requirements to be met by deploying many smaller distributed array nodes, rather than a single large array. However, with these advantages comes stringent time, frequency, and phase coordination requirements between nodes in the array [3], [4]. For modulated waveforms, such as pulse compressed ranging waveforms, or information carrying waveforms, timing synchronization becomes increasingly important [5].

While other works have covered the topics of distributed wireless beamforming [6]–[9], these works have all focused on frequency-only synchronization, or low bandwidth synchronization with timing synchronization on the order of nanoseconds, limiting throughput to sub-gigabaud speeds. To achieve high coherent gain at large modulation bandwidths, required for high data-rate communications and high range resolution radar waveforms, timing synchronization must be a small fraction of the waveform period at the highest frequency of modulation [5]. For example, for a symbol rate of $1\,\mathrm{GBd}$ modulation bandwidth, to achieve greater than 90% coherent gain at the target, the timing synchronization would need to be below $67\,\mathrm{ps}$, assuming perfect frequency and phase coherence.

In this work, we present experimental demonstrations of a distributed wireless time-frequency synchronization system using high accuracy spectrally sparse two-tone waveforms for time synchronization and a two-tone self-mixing circuit for wireless frequency syntonization. We show demonstrate beamforming to a target at a range of $41\,\mathrm{m}$ in a cluttered outdoor environment with a time transfer standard deviation of $36.7\,\mathrm{ps}$ and a beamforming alignment standard deviation of $27.6\,\mathrm{ps}$.

II. High Accuracy Synchronization

To achieve high bandwidth coherent distributed array operation, the systems must be tightly synchronized in frequency, phase, and time. A common metric for evaluating the overall system performance is the probability of achieving a certain coherent gain value $P(G_c > X)$; commonly, a G_c value of 0.9 is chosen $G_c > 0.9$, i.e., 0.5 dB less than the ideal coherent gain with perfect phase alignment. This translates to phase accuracies of below $18°$ to achieve $P(G_c > X) \geq 0.9$, where λ is the carrier wavelength [3]. For timing synchronization, the alignment requirements are waveform dependent; continuous-wave (CW) amplitude modulated waveforms may achieve $P(G_c > X) \geq 0.9$ by simply achieving 90% overlap, however for continuously phase-modulated waveforms such as the linear frequency modulation (LFM) waveform the timing requirements are considerably more stringent, typically resulting in overlap requirements of $\ll 1\%$ of the signal duration, for typical chirp-rates [5], thus very high accuracy synchronization is required for wide-band modulations.

In general, the local time at each node in a system of N wireless nodes with independent clocks can be modeled as

$$T_n(t) = t + \delta_n(t) + \nu_n(t) \tag{1}$$

where $\delta_n(t)$ is a time-varying offset from the global true time, and $\nu_n(t)$ is a zero-mean time-varying noise term due to device noise from all components in the timing chain [10, chapter 10.1]. The goal of timing synchronization is to determine the offset $\delta_n(t)$ of each node. For simplicity, it may be assumed

that node 0 has the true time; thus, we must correct offset relative to node 0, i.e., $\Delta_{0n} = \delta_0 - \delta_n$, where $\delta_0 = 0$.

To estimate this offset, a two-way time transfer (TWTT) technique, described in [11], is used based on the assumptions that the channel is quasi-static during the synchronization epoch, and the systems are syntonized (aligned in frequency). The synchronization process begins when node n transmits a ranging waveform to node 0 which it locally timestamps at $T_n(t_{\mathrm{TX}n})$ which we will denote as $T_{\mathrm{TX}n}$ for brevity. Node 0 will timestamp the received waveform with its local time $T_{\mathrm{RX}0}$ and will then respond with another locally timestamped ranging waveform at $T_{\mathrm{TX}0}$ after some arbitrary processing delay τ_{proc}. Finally, node n will timestamp the received waveform at $T_{\mathrm{RX}n}$ and estimate its offset Δ_{0n} using

$$\Delta_{0n} = \frac{(T_{\mathrm{RX}0} - T_{\mathrm{TX}n}) - (T_{\mathrm{RX}n} - T_{\mathrm{TX}0})}{2}. \tag{2}$$

To estimate the time offset to a high accuracy, the one-way time delay estimates must also be high accuracy. To accomplish this, we use the two-tone waveform, which is an approximately optimal time-delay estimation waveform that maximizes the mean-squared-bandwidth of the waveform, thus minimizing the Cramer-Rao lower bound for a constant signal-to-noise ratio (SNR) and bandwidth [12]. A matched filter in the form of $s_{\mathrm{MF}}[n] = s_{\mathrm{RX}}[n] \circledast s^*_{\mathrm{TX}}[-n]$, where s_{TX} and s_{RX} are the TX and TX waveforms respectively, is then applied to the received waveform which maximizes the power at the output of the filter in the time delay bin corresponding to the true time delay of the received waveform. This results in approximately a cosine squared function with a period equal to the period of the tone separation, windowed by a triangular function with duration of twice the time transfer pulse duration τ_p. Because the spacing of the samples in the matched filter output, for typical analog to digital converter rates, the time resolution will still be much coarser than desired, and an interpolation step must then be applied. In this work, we use a quadratic least-squares (QLS) fitting process due to its efficient closed-form solution given three points of the waveform. The quadratic function approximates the shape of a single lobe around the peak the matched filter [13], [14, Chapter 7.2]. After interpolation, due to the approximate nature of the quadratic function to the peak of the matched filter lobe, there remains a small residual bias; because this is a deterministic characteristic of the ranging waveform and sample rate, which are known a priori, a pre-computed lookup table is used to compensate for the bias based on the QLS estimate.

III. Experimental Configuration

To validate the time and frequency transfer techniques in a real-world environment, the system was placed in a cluttered outdoor courtyard. The full system schematic and experimental setup are shown in Figs. 1 and 2. The nodes were separated by a distance of $2.1\,\mathrm{m}$ and the beamforming target was placed $41\,\mathrm{m}$ downrange. For this experiment, a Keysight DSOS804A $20\,\mathrm{GSa/s}$ oscilloscope was used with a 10-dBi L-Com HG72710LP-NF log-periodic antenna as the ranging target, pictured in the inset of Fig. 2, to digitize the waveforms at the carrier and estimate the time delay, phase, and coherent gain of the beamforming pulses. Each array node had a single Ettus Research X310 SDR with two UBX-160 daughterboards each to perform the time transfer and beamforming; the SDRs were configured to operate at $200\,\mathrm{MSa/s}$ and transmitted two-tone waveforms with $40\,\mathrm{MHz}$ tone separation for time transfer, and orthogonal $40\,\mathrm{MHz}$ LFMs for beamforming accuracy estimation, described in Section IV. The cart used for node 0 contained a desktop PC running GNU Radio to control the SDRs; the secondary node SDR was connected via a long fiber-optic cable for sending control signals, however a wireless link could be used. Each node had two antennas, one 8-dBi L-Com HG2458-08LP-NF log-periodic used for time transfer, and one 10-dBi L-Com HG72710LP-NF log-periodic antenna used for beamforming (the same as the target). SDR channel 0 on each node was connected to an Analog Devices EV1HMC849ALP4C transmit-receive switch, controlled by the time-transfer direction, which was connected to a power combiner/splitter and finally an antenna used for time and frequency transfer.

A one-way wireless frequency transfer circuit, described in [7], was used to syntonize the platforms. This technique provides a $10\,\mathrm{MHz}$ frequency reference using two tones modulated onto a carrier frequency spaced $10\,\mathrm{MHz}$ apart. Once it is received, the signal is split and mixed with a copy of itself, and then low-pass filtered resulting in only a signal at the frequency of the tone separation, in this case, $10\,\mathrm{MHz}$. This two-tone signal was generated at node 0 at a carrier of $4.3\,\mathrm{GHz}$ by a Keysight E8267D and connected to the second side of the splitter. The reference $10\,\mathrm{MHz}$ output of the signal generator was then connected to SDR 0 so they were frequency locked. The two-tone signal was received at node 1 and split into the two-tone self-mixing frequency locking circuit to produce a single $10\,\mathrm{MHz}$ square wave which SDR 1 was locked to, to ensure the same frequency reference as SDR 0.

Finally, because the nodes have random initial start times, the nodes must first be coarsely time aligned to ensure the $30\,\mu\mathrm{s}$ transmit and receive windows for the high-accuracy pulses will overlap. To accomplish this, a single pulse-per-second (PPS) pulse from a global navigation satellite system (GNSS) reference is used to align the system clocks on the order of ten to one hundred nanoseconds at system initialization—the PPS signal is not used afterwards. From here, the system exchanges $\tau_p = 30\,\mu\mathrm{s}$ two-tone pulses centered in a $30\,\mu\mathrm{s}$ window to perform the time offset correction described in Section II.

IV. Experimental Results

To characterize system performance, the beamforming waveforms were chosen to be two orthogonal LFM waveforms—an up-chirp and a down-chirp; this provides the ability to determine time delay and phase of each platform, shown in Fig. 3. The initial inter-node beamforming bias was used to calibrate the time-of-flight difference due to beamforming angle. From these, the standard deviation of each quantity was also calculated to evaluate accuracy, shown in

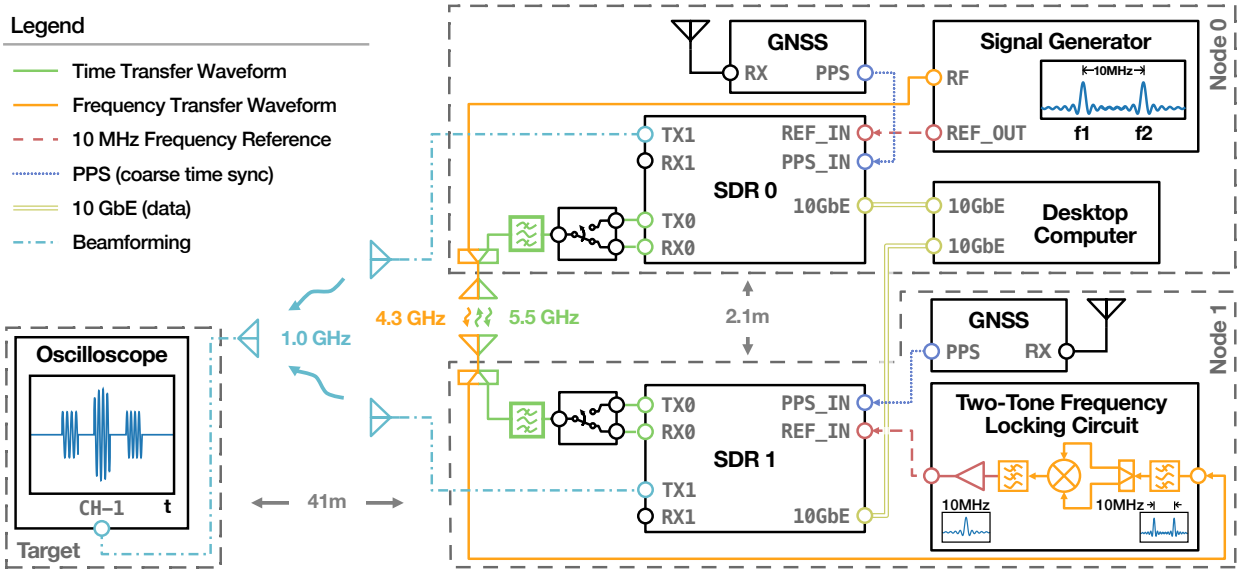

Fig. 1. System schematic showing target node (left), and distributed array nodes 0 and 1 (top and bottom, respectively). Node 0 held the coordination computer running GNU Radio which was connected via 10 GbE to each node for control. Node 0 also contained the signal generator for frequency reference which generated a 10 MHz two-tone waveform at 4.3 GHz to be transmitted to the two-tone frequency locking circuit on node 1 used to lock SDR 1, as well as generated the 10 MHz frequency reference for the SDR on node 0. Each node also contained a GNSS receiver for coarse initial time synchronization between platforms (only used once on initialization). Finally, channel 0 on each SDR was connected to a transmit-receive switch to controlled via timing synchronization pulse direction which was connected to the 8-dBi log-periodic time-frequency transfer antennas, and channel 1 on each SDR was connected to a 10-dBi log-periodic beamforming antenna.

Fig. 2. Experimental configuration of the distributed beamforming system in a fully enclosed courtyard. Node 0 is on the left and node 1 is on the right, separated by 2.1 m. The ranging target, shown in the inset is located 41 m downrange, below the blue walkway. A 20 GSa/s sampling oscilloscope was used to digitize the waveforms at the carrier to estimate time delay, phase, and coherent gain at the beamforming location.

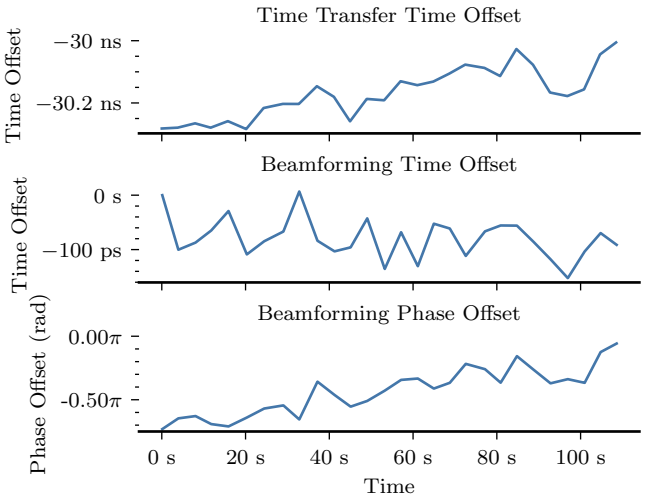

Fig. 3. (Top) Time offset measured between the two systems Δ_{0n} after coarse synchronization using GNSS PPS. We estimate Δ_{0n} using a TWTT exchange, and correct for it by delaying the samples at node 1 accordingly. (Middle) Time offset of the beamformed signals after delay correction using (2). (Bottom) Phase offset measured at the beamforming target after delay correction using (2). Although the system clocks skew by ∼280 ps over the duration of the experiment, the beamforming signal only varies by at most 160 ps.

Fig. 4; the standard deviation was computed over a ten-sample moving window. Because the cycle rate was ∼4 s, the accuracy plot starts at ∼40 s into the 110 s experiment windows. From Fig. 4 it is shown that over the duration of the experiment, the time transfer synchronization accuracy reached a minimum of 36.7 ps with an SNR of ∼21 dB while the beamforming reached an accuracy of 27.6 ps. The beamforming is expected to have a lower standard deviation as it is run directly after (∼300 ms) the system performs a time alignment. The phase stability was also measured, shown in the bottom row of Fig. 4, which was $\sim 0.1\pi$ radians, or ∼18°. Based on the beamforming delay and phase accuracies, this implies the system should be capable of transmitting data with a data modulation bandwidth of up to 2.415 GBd and maintaining a carrier frequency of up to 1 GHz with $P(G_c > 0.9) \geq 0.9$.

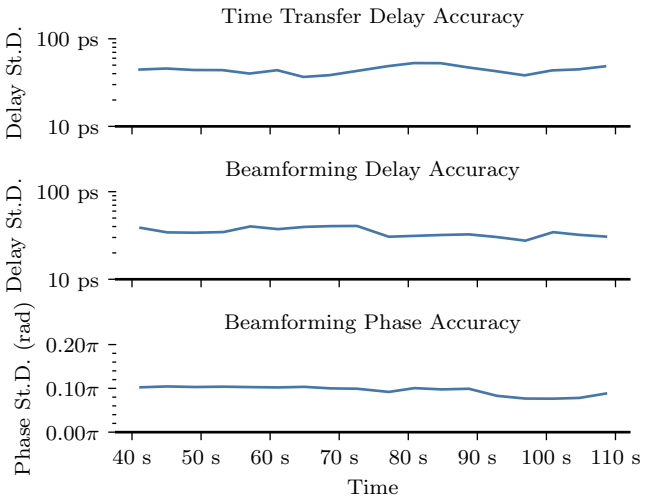

Fig. 4. Time standard deviation measured between the two systems (top) and time and phase standard deviation measured at the beamforming target (middle and bottom).

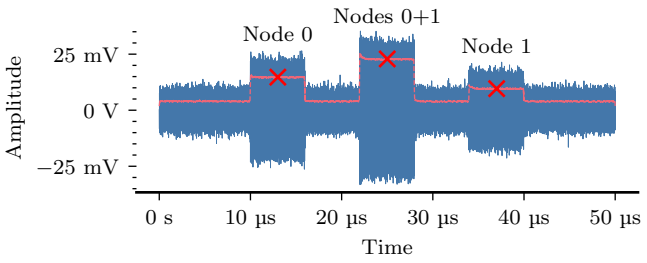

Fig. 5. Coherent summation of CW pulses from two nodes. First and third pulses are from nodes 0 and 1 respectively, second pulse is the summation of both nodes. The pink dashed line indicates the smoothed signal envelope, and the red $\times$ marks indicate the sample location for the coherent gain estimation, found to be 95.4%.

Finally, to demonstrate the beamforming performance of the system, a set of coherent pulse measurements were performed after the system was aligned, shown in Fig. 5. Each node transmitted two $6\,\mu$s pulses separated by $6\,\mu$s with the center pulse being overlapped; the sharp rising edge indicates a high level of time alignment. The power level indicates the phase coherence of the system which was estimated by first taking the magnitude of Hilbert transform of the RF waveform to find the signal envelope, then performing a $50\,$ns low-pass moving average, plotted as a dashed pink line in Fig. 5. The coherent gain was computed by taking the ratios of the power levels at the center of each pulse, indicated by the $\times$ marks in Fig. 5. For the given measurement, the coherent gain was determined to be $G_c = 0.954$.

V. Conclusion

In this paper, a fully wireless two node distributed time-frequency synchronization system for distributed phased array beamforming is demonstrated. A coherent gain of greater than 0.9 is achieved at the beamforming frequency of $1\,$GHz with a beamforming timing synchronization accuracy of $36.7\,$ps enabling symbol rates of up to $2.415\,$GBd.

References

[1] "2015 NASA technology roadmaps," National Aeronautics and Space Administration, Tech. Rep., July 2015.

[2] "2020 NASA technology taxonomy," National Aeronautics and Space Administration, Tech. Rep. HQ-E-DAA-TN76545, Jan. 2020.

[3] J. A. Nanzer, R. L. Schmid, T. M. Comberiate, and J. E. Hodkin, "Open-loop coherent distributed arrays," *IEEE Trans. Microw. Theory Techn.*, vol. 65, no. 5, pp. 1662–1672, 2017.

[4] J. A. Nanzer, S. R. Mghabghab, S. M. Ellison, and A. Schlegel, "Distributed phased arrays: Challenges and recent advances," *IEEE Trans. Microw. Theory Techn.*, vol. 69, no. 11, pp. 4893–4907, 2021.

[5] P. Chatterjee and J. A. Nanzer, "Effects of time alignment errors in coherent distributed radar," in *2018 IEEE Radar Conference (RadarConf18)*, 2018, pp. 0727–0731.

[6] P. Bidigare, M. Oyarzyn, D. Raeman, D. Chang, D. Cousins, R. O'Donnell, C. Obranovich, and D. R. Brown, "Implementation and demonstration of receiver-coordinated distributed transmit beamforming across an ad-hoc radio network," in *2012 Conference Record of the Forty Sixth Asilomar Conference on Signals, Systems and Computers (ASILOMAR)*, 2012, pp. 222–226.

[7] S. R. Mghabghab and J. A. Nanzer, "Open-loop distributed beamforming using wireless frequency synchronization," *IEEE Trans. Microw. Theory Techn.*, vol. 69, no. 1, pp. 896–905, 2021.

[8] H. Ouassal, M. Yan, and J. A. Nanzer, "Decentralized frequency alignment for collaborative beamforming in distributed phased arrays," *IEEE Trans. Wireless Commun.*, vol. 20, no. 10, pp. 6269–6281, 2021.

[9] K. Alemdar, D. Varshney, S. Mohanti, U. Muncuk, and K. Chowdhury, "RFClock: timing, phase and frequency synchronization for distributed wireless networks," in *Proceedings of the 27th Annual International Conference on Mobile Computing and Networking*, 2021, pp. 15–27.

[10] D. Pozar, *Microwave Engineering*, 3rd ed. John Wiley & Sons, Inc., 2005.

[11] J. M. Merlo, S. R. Mghabghab, and J. A. Nanzer, "Wireless picosecond time synchronization for distributed antenna arrays," *IEEE Transactions on Microwave Theory and Techniques*, pp. 1–12, 2022.

[12] J. A. Nanzer and M. D. Sharp, "On the estimation of angle rate in radar," *IEEE Trans. Antennas Propag.*, vol. 65, no. 3, pp. 1339–1348, 2017.

[13] R. Moddemeijer, "On the determination of the position of extrema of sampled correlators," *IEEE Trans. Signal Process.*, vol. 39, no. 1, pp. 216–219, 1991.

[14] M. Richards, *Fundamentals of Radar Signal Processing, Second Edition*. McGraw-Hill Education, 2014.